Chem Biol Drug Des 2015; **85:** 534–540

Research Article

Hydrogen-Bonded His93 As a Sensitive Probe for Identifying Inhibitors of the Endocannabinoid Transport Protein FABP7

Sergiy Tyukhtenko[1], Karrie Chan[1], Rubin Jiang[1], Han Zhou[1], Richard W. Mercier[1], De-Ping Yang[2], Alexandros Makriyannis[1] and Jason J. Guo[1,*]

[1]Center for Drug Discovery, Department of Pharmaceutical Sciences and Department of Chemistry and Chemical Biology, Northeastern University, 360 Huntington Avenue, Boston, MA 02115, USA
[2]Physics Department, College of the Holy Cross, 1 College Street, Worcester, MA 01610, USA
**Corresponding author: Jason J. Guo, j.guo@neu.edu*

The human brain FABP (FABP7) has been shown to be an intracellular carrier protein that can significantly potentiate the uptake of the endocannabinoid anandamide. For this reason, there is a great interest in the discovery and development of FABP7 inhibitors for treating stress, pain, inflammation, and drug abuse. We found that in the ^{1}H-NMR spectrum of the protein, a well-separated downfield resonance arising from the hydrogen-bonded His93 side chain is very sensitive to ligand binding. Using this characteristic spectral marker together with another well-resolved upfield resonance from the side chain of Val84, we have identified that an adipocyte FABP (FABP4) inhibitor BMS309403 also binds tightly to FABP7. Our data demonstrated that this unique His93 downfield resonance can be used as a sensitive probe for rapidly and unambiguously identifying novel high-affinity FABP7 ligands. The findings should help accelerate the discovery of potential drug leads for the modulation of endocannabinoid transport.

Key words: anandamide transport, endocannabinoids, fatty acid binding protein, NMR

Abbreviations: AA, arachidonic acid; AEA, anandamide, *N*-arachidonoylethanolamide; DHA, docosahexaenoic acid; FABP7, fatty acid binding protein 7, brain fatty acid binding protein; HSQC, heteronuclear single quantum coherence; OA, oleic acid.

Received 20 August 2014, revised 18 September 2014 and accepted for publication 19 September 2014

Anandamide (*N*-arachidonoylethanolamide, AEA) is the first endocannabinoid isolated from porcine brain (1) that binds to the human cannabinoid receptor and stimulates receptor-mediated signal transduction (2). The biosynthesis and physiology of AEA are well understood (3,4), but its mechanism of uptake has been elusive. Despite intensive studies on the AEA transport process (5–9), the question remains on how the uncharged lipophilic endocannabinoid ligand AEA crosses the cellular membrane to access the hydrophilic cytosol. Recently, it was reported (10,11) that a group of carrier proteins, particularly fatty acid binding proteins (FABPs), can significantly enhance the cellular uptake and subsequent inactivation of AEA. The findings provide a potential new therapeutic modality to the treatment of pain, inflammation, and drug abuse through dual inhibition of the deactivating enzymes such as fatty acid amide hydrolase (FAAH) (12) and the endocannabinoid transport proteins.

FABPs are intracellular lipid chaperones that exhibit unique patterns of tissue expression and are expressed most abundantly in tissues involved in active lipid metabolism (13). Human brain FABP (FABP7), which has been shown to significantly potentiate AEA uptake (10), is expressed in various regions in the brain and is distinguished from other FABPs by its strong affinity for polyunsaturated fatty acids (14,15). Currently only a few specific FABP inhibitors have been described (16,17), and there are no selective ligands available for FABP7. In this work, we sought to obtain structural insights on the FABP7 binding pocket due to a growing interest in the discovery and development of selective FABP7 inhibitors (18). We found that in the 1D ^{1}H-NMR spectrum, a well-separated downfield resonance arising from the hydrogen-bonded His93 side chain is very sensitive to ligand binding. Using this characteristic spectral marker, we have successfully demonstrated that a selective adipocyte FABP (FABP4) inhibitor (16) BMS309403 also binds tightly to FABP7. Thus, this unique His93 can be exploited as a sensitive probe for NMR-based high-throughput screening to rapidly identify novel FABP7 ligands that can subsequently be developed into selective probes or drug leads.

Methods and Materials

Chemicals

Docosahexaenoic acid (DHA), arachidonic acid (AA), oleic acid (OA), and all other common chemicals were purchased from Sigma-Aldrich (St. Louis, MO, USA). Three of the four representative cannabinoid ligands, Δ^9-tetrahy-

© 2014 John Wiley & Sons A/S. doi: 10.1111/cbdd.12440

drocannabinol (Δ^9-THC), CP55940 (2-[(1R,2R,5R)-5-hydroxy-2-(3-hydroxypropyl)cyclohexyl]-5-(2-methyloctan-2-yl)phenol), and SR141716A (rimonabant; 5-(4-Chlorophenyl)-1-(2,4-dichloro-phenyl)-4-methyl-*N*-(piperidin-1-yl)-1*H*-pyrazole-3-carboxamide), were obtained from the National Institute on Drug Abuse (NIDA). The cannabinoid ligand WIN55212-2 ((R)-(+)-[2,3-Dihydro-5-methyl-3-(4-morpholinylmethyl)pyrrolo[1,2,3-de]-1,4-benzoxazin-6-yl]-1-napthalenylmethanone) was purchased from Tocris Bioscience (R&D Systems, Minneapolis, MN, USA). The selective adipocyte FABP (FABP4) inhibitor, BMS309403 (2-[2′-(5-Ethyl-3,4-diphenyl-1*H*-pyrazol-1-yl)biphenyl-3-yl-oxy]-acetic acid), was purchased from EMD Chemicals (San Diego, CA, USA). The [9, 10-^{3}H] oleic acid and Lipidex 1000 resin used for the radioactive competition binding assay were from Perkin Elmer (Waltham, MA, USA).

Expression, purification, and refolding of human brain FABP

Human FABP7 encoding *c*DNA in pCMV6-XL5 was purchased from OriGene (Rockville, MD, USA). The Champion pET directional TOPO expression kit from Invitrogen was employed for subcloning and expression in BL21 *E. coli* cells. The recombinant FABP7 contained a polyhistidine tag at the N-terminus (12 additional amino acids) that allowed single-step purification by immobilized cobalt affinity chromatography. Extraction from inclusion bodies and His-tag purification were performed under strong denaturing condition using 8 M urea. The purified FABP7 was first refolded in a cold refolding buffer (1 M arginine, 5 mM DTT, 150 mM NaCl, 20 mM PBS, pH 7.4) followed by dialysis against NMR buffer (10 mM PBS, 100 mM NaCl, 1 mM DTT, and 0.05% sodium azide, pH 7.4) using Spectra/Por dialysis membrane (MWCO 6–8 K) and further delipidated over a Lipidex 1000 column at 37 °C according to a reported procedure (19). Uniformly ^{15}N-enriched FABP7 protein was obtained by first growing cells in an M9 minimal medium containing 1 g/L of $^{15}NH_4Cl$ (Cambridge Isotope Laboratories, Andover, MA, USA) followed by the same purification and refolding protocol as above.

High-resolution NMR experiments

All one- and two-dimensional high-resolution NMR experiments were conducted at 298 K on a Bruker AVANCE*II* 700 MHz NMR spectrometer. The 1D ^{1}H-NMR spectra of the human recombinant FABP7 were acquired using a WATERGATE 3-9-19 scheme with a water flipback (Bruker pulse sequence: p3919fpgp) pulse to minimize solvent saturation transfer. For 2D ^{1}H-^{15}N correlation, a fast heteronuclear single quantum coherence (Fast-HSQC) detection scheme (20,21) was employed. To study ligand binding, NMR titration experiments were performed to monitor complex formation. All ligands were first dissolved in dimethyl sulfoxide-d_6 (DMSO-d_6) to create concentrated stock solutions. The final concentration of DMSO-d_6 in the protein–ligand solution did not exceed 2% (v/v).

Lipidex competition binding assay

Ligand binding to purified human FABP7 was analyzed by the Lipidex assay (14,15,19). Briefly, 2.5 μM of purified and delipidated recombinant FABP7 protein was incubated with the same concentration of oleic acid at a constant hot to cold ratio of 1:50 at 37 °C for 15 min. Solutions with different competitor concentrations were subsequently added followed by an additional 30 min incubation at 37 °C. The mixtures were cooled on ice for 15 min, and 50 μL of a 50% (v/v) precooled Lipidex 1000 suspension was added with subsequent vortexing for 15 min while maintaining the temperature below 4 °C to remove any free oleic acid from the mixture. Raw data for constructing the competition binding curve were obtained by separation of protein-bound and free fatty acid (Lipidex bound) by vacuum filtration using Pall 96-well filter plates (0.45 μm pore size) and scintillation counting of the protein-bound fractions.

Results and Discussion

The 1D ^{1}H-NMR spectrum of human FABP7 (Figure 1A) is substantially crowded with severe overlapping in the entire amide, aromatic, and aliphatic regions. However, two distinctive peaks can be readily identified: one at the far downfield region (> 11 ppm) and the other at the high

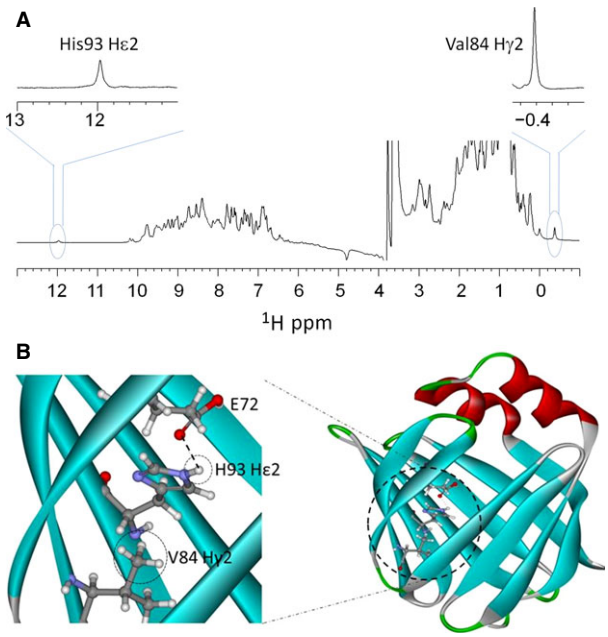

Figure 1: (A) One-dimensional ^{1}H-NMR spectrum of human recombinant FABP7. Two very distinctive peaks, one located at the far downfield region (> 11 ppm) and the other at the upfield region (< 0 ppm), are highlighted. (B) Strong H-bond between the His93 Hε2 and the side chain carboxyl group of Glu72 in the binding pocket of FABP7. The Val84 Hγ2 protons experience strong shielding by the ring current from the His93 imidazole side chain.

upfield region (< 0 ppm). These two peaks can be assigned unambiguously based on earlier NMR structural studies of FABP7 (PDB ID: 1JJX) (22,23). The peak at 11.96 ppm is assigned to Hε2 of the His93 residue, while the peak at −0.38 ppm is assigned to the Hγ2 of Val84. The strong downfield shift of the His93 Hε2 proton can be attributed to a hydrogen bonding interaction with the side chain carboxyl group of Glu72 (22) (Figure 1B). Additionally, the ring current from the His93 imidazole side chain causes a significant upfield shift to the Hγ2 protons of Val84 which is residing on a separate β-strand. As the hydrogen-bonded His93 residue is located within the binding pocket, we hypothesized that it will be sensitive to ligand binding and may serve as a characteristic spectral marker for ligand screening.

We first examined changes of this characteristic His93 downfield resonance in the presence of a group of natural fatty acids. FABP7 is distinguished from other FABPs by its strong affinity for unsaturated fatty acids including docosahexaenoic acid, arachidonic acid, and oleic acid with K_i values of 30, 250 and 440 nM, respectively (15). Figure 2 shows three representative series of NMR titration spectra from samples containing 120 μM FABP7 with various concentrations of DHA, AA, or OA. For FABP7 in its *apo* form, there is only one characteristic peak in the far downfield region of the ^{1}H-NMR spectrum. Addition of increasing amounts of DHA or AA to the protein solution leads to a gradual decrease of the His93 Hε2 peak at 11.96 ppm, while a new peak appears and becomes progressively more intense at 11.90 or 12.02 ppm when titrating with DHA or AA, respectively. At a protein to ligand molar ratio of 1:3, the 11.96 ppm peak completely disappears indicating that the FABP7 protein binding pocket is now fully occupied by docosahexaenoic acid or arachidonic acid. In parallel with the above, we also observed a very broad and gradually increasing peak at 11.24 ppm during the titration with AA but not with DHA, which we speculate may be due to a new hydrogen bond formation. Titration experiments with OA produced a somewhat different result with the His93 Hε2 peak gradually shifting from 11.96 to 11.92 ppm but with no new peaks appearing in the spectrum. This suggests a fast exchange process on the NMR time scale and reflects a relatively lower binding affinity of oleic acid.

The robustness of this characteristic His93 as a spectral marker for ligand binding was further studied using a number of non-lipid ligands including four representative cannabinoid ligands Δ^9-THC, CP55940, WIN55212-2, and SR141716A, and an adipocyte FABP (FABP4) inhibitor BMS309403 (Figure 3A). Figure 3B shows a series of ^{1}H-NMR spectra of FABP7 in the presence of one or more of these ligands at protein to ligand ratios of 1:4. As stated above, the ^{1}H-NMR spectrum of FABP7 in its *apo* form only gives rise to one single sharp peak (11.96 ppm) in the far downfield region. After additions of one or more of the cannabinoid ligands, we did not observe any discernible changes to this characteristic downfield resonance. This suggests that there is no binding between any of the four cannabinoid ligands to the FABP7 protein. However, after adding the BMS309403 ligand, the 11.96 ppm peak almost completely disappears accompanied by the emergence of three intense peaks at 11.67, 11.55, and 11.27 ppm. We conclude that of the five non-lipid ligands tested, only the adipocyte FABP (FABP4) inhibitor BMS309403 binds to FABP7.

To further explore the binding characteristics of BMS309403 with the FABP7 protein, we performed a detailed titration study by adding various amounts of the ligand into the FABP7 protein solution. Figure 4 shows a series of NMR titration spectra from samples with different concentrations of BMS309403 in 120 μM FABP7 solutions. In its *apo* form, FABP7 gives rise to only one characteristic 11.96 ppm peak in the far downfield region of the ^{1}H-NMR spectrum. Addition of BMS309403 leads to the appearance of three gradually increasing peaks at 11.67, 11.55, and 11.27 ppm, which are accompanied by the gradual disappearance of the original 11.96 ppm peak

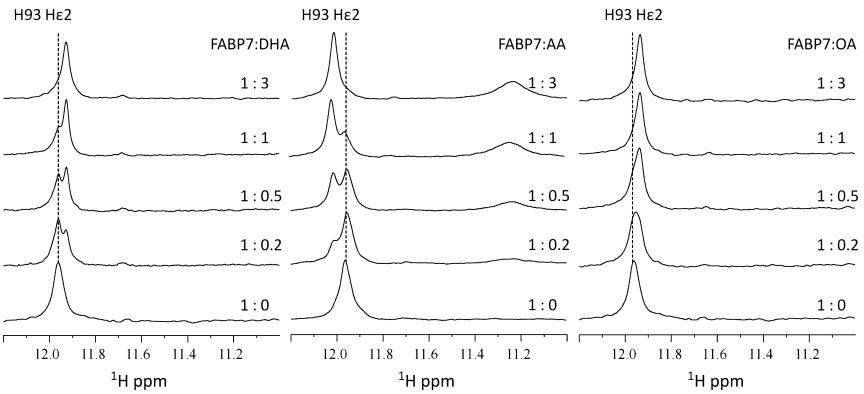

Figure 2: Downfield region of the ^{1}H-NMR spectra of FABP7 titrated with docosahexaenoic acid (DHA) (left), arachidonic acid (AA) (middle), or oleic acid (OA) (right). The protein to ligand molar ratios are indicated in each spectrum.

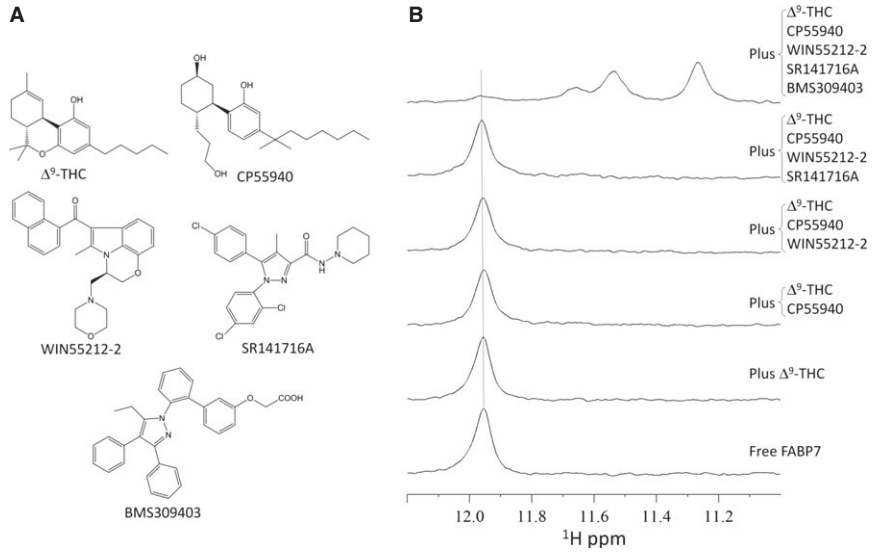

Figure 3: (A) Structures of four representative cannabinoid ligands: Δ^9-THC, CP55940, WIN55212-2, and SR141716A, and a non-lipid adipocyte FABP (FABP4) inhibitor BMS309403. (B) Downfield region of the ^{1}H-NMR spectra of FABP7 with the additions of Δ^9-THC, CP55940, WIN55212-2, SR141716A, and BMS309403. The protein to ligand ratios are 1:4.

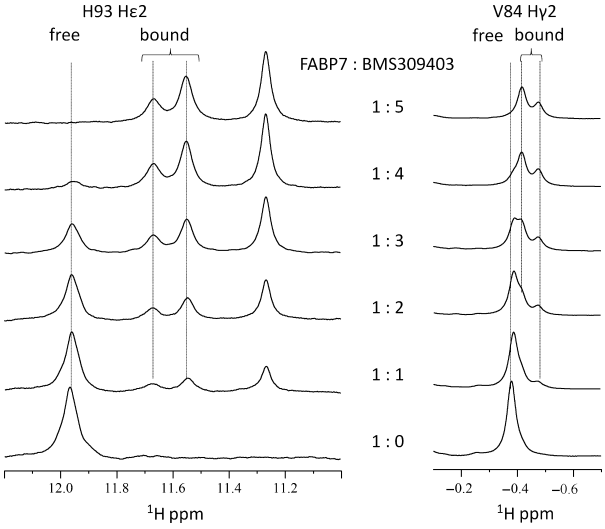

Figure 4: Downfield (left) and upfield (right) regions of the ^{1}H-NMR spectra of FABP7 titrated with BMS309403. The protein to ligand molar ratios are indicated in each spectrum.

from the *apo* protein sample. Interestingly, during the titration experiment, there was no change in the frequencies of these new peaks or the original 11.96 ppm peak. This provides evidence of a tight binding of BMS309403 to FABP7 with slow dissociation of the ligand–protein complex. We assigned both the 11.67 and 11.55 ppm peaks to the His93 Hε2 proton. Our assignment is supported by the observation that the integral value of these two peaks from the spectrum due to the ligand–protein complex (top left in Figure 4) is identical to that of the 11.96 ppm peak from the *apo* protein (bottom left in Figure 4). The upfield resonance (−0.38 ppm) from the Val84 Hγ2 protons shows a very similar profile. In the spectrum from ligand–protein complex (top right in Figure 4), the −0.38 ppm peak is completely replaced by two new peaks at −0.43 and −0.50 ppm, both of which can be assigned to the Val84 Hγ2 protons. Thus, our data clearly demonstrate that the characteristic spectral markers arising from the His93 Hε2 as well as the Val84 Hγ2 protons are very sensitive to binding of the BMS309403 ligand.

To confirm the NMR spectral assignments upon binding of the BMS309403 ligand, we performed two-dimensional ^{1}H-^{15}N heteronuclear single quantum coherence (HSQC) experiments on uniformly ^{15}N-labeled FABP7 in the absence or presence of various concentrations of BMS309403. The HSQC spectrum from the *apo* protein sample (Figure 5A) shows that the 11.96 ppm peak correlates with a nitrogen resonance at 163.2 ppm, which corroborates that this downfield peak is indeed arising from the Hε2 proton of His93. At a protein to ligand molar ratio of 1:1, only two additional peaks at 11.67 and 11.55 ppm appear within this spectral range (Figure 5B bottom panel). This observation provides evidence that both the 11.67 and 11.55 ppm peaks are indeed due to the Hε2 proton of His93. We speculate that the 11.27 ppm peak, which cannot be attributed to an N-H proton, is due to a new hydrogen bond formed between the phenolate group of Tyr128 and the ligand carboxylic acid. The above results also suggest that the FABP7/BMS309403 complex exists in two distinct conformations which can be distinguished by monitoring the His93 Hε2 resonance.

We further determined the binding affinity of BMS309403 to FABP7 using the Lipidex competition binding assay

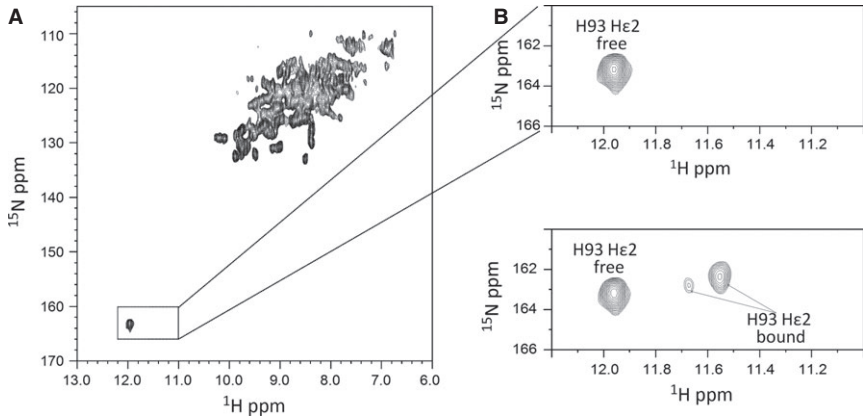

Figure 5: (A) 2D ^{1}H-^{15}N HSQC spectrum of uniformly ^{15}N-enriched FABP7 protein. (B) Partial ^{1}H-^{15}N HSQC spectrum highlighting the N-H resonances from histidine side chains of FABP7 in the absence (top) or presence (bottom) of BMS309403.

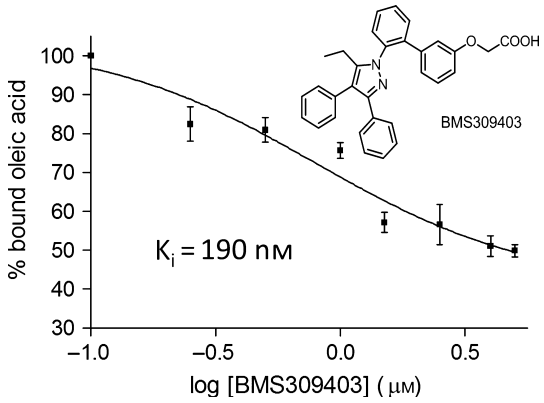

Figure 6: Competitive binding of BMS309403 and [9,10-^{3}H] oleic acid to the FABP7 protein using the Lipidex 1000 assay.

(14,15,19). Due to the lack of high-affinity FABP7 ligands, it is challenging to select a proper radioactivity ligand and implement the standard competition binding assay protocol. As with earlier studies (14,15), we used [9,10-^{3}H] oleic acid as a radioligand to study the binding of ligands to FABP7, and all experiments were conducted with comparable ligand and protein concentrations using 96-well plates. We have obtained competition binding curves for a number of ligands as exemplified in Figure 6 with BMS309403. To convert the experimentally obtained IC_{50} to a K_i value, however, we could not rely on the widely used Cheng–Prusoff equation (24) because the experiments were performed with significantly higher concentrations of protein in which the IC_{50} for a ligand depends on the concentrations of the protein as well as the radioligand used. For this reason, we used the method developed by Nikolovska-Coleska *et al.* (25) to take into account the concentrations of both the protein and radioligand, and we found that the K_i for BMS309403 to FABP7 is 190 nM.

We have now demonstrated that the His93 Hε2 resonance in the 1D ^{1}H-NMR spectrum from FABP7 is well separated and is very sensitive to ligand binding. As His93 is located directly within the FABP7 binding pocket, changes in its chemical shift and/or linewidth may be attributed to specific ligand–protein interactions. Therefore, His93 can be used as a characteristic spectral marker to conduct NMR-based high-throughput screening aimed at rapidly identifying high-affinity FABP7 inhibitors. This method may be directly applied to identify ligands for other fatty acid binding proteins including the heart, adipocyte, and testis FABPs (FABP3, FABP4, and FABP9) in which this histidine residue is conserved (26) and presumably hydrogen bonded. However, it is worth noting that we were not able to find this particular H-bond from representative crystal structures of these three FABPs (PDB IDs: 1HMS, 2NNQ, and 4A60) (27–29). As a matter of fact, we also examined the two available crystal structures of FABP7 (PDB IDs: 1FDQ and 1FE3) (14), but we were not able to find this particular H-bonding interaction involving the His93 side chain. This is not surprising as X-ray crystallography often cannot recognize the exact protonation and rotameric states of histidine residues resulting in the common ambiguities in crystal structures (30). Therefore, analysis of the involvement of histidine residues in hydrogen bonding with proximal donors or acceptors should be taken with precaution. The advantage of NMR is that proton nucleus can be directly detected. In fact, in an earlier NMR work on FABP3 (31), it was reported that the His93 Hε2 resonance is at 11.11 ppm indicating that the imidazole ring is involved in H-bonding. It would be interesting to further examine for the presence of the hydrogen-bonded His93 from the downfield region of the ^{1}H-NMR spectra of the other two FABPs.

Comparing to most of the ligand-based NMR screening techniques, our protein-based method has the advantage of yielding minimal false-positive results. Additionally, unlike most of the protein-based NMR approaches, our method uses only the 1D ^{1}H-NMR spectra of proteins and therefore does not require isotopic labeling of the protein under investigation. Isotopic labeling of proteins is often costly

and time-consuming, and places limitations on the usefulness of the method. Further, to take advantage of the expected low level of false positives, this method can be first applied to screen mixtures of compounds or combinatorial libraries. After detection of binding, we can use one of the ligand-based screening methods such as 1D saturation transfer difference (STD) (32,33) or $T_{1\rho}$-relaxation filter experiments (34,35) to obtain the identity of the bound ligand without any need to deconvolute the mixture.

Conclusions

We have shown that a well-separated downfield ^{1}H-NMR resonance arising from the hydrogen-bonded His93 side chain of FABP7 is very sensitive to ligand binding. Using this characteristic spectral marker, we have successfully identified that a selective adipocyte FABP (FABP4) inhibitor BMS309403 also binds tightly to FABP7. This unique spectral marker can be employed to conduct NMR-based high-throughput screening for rapidly and unambiguously identifying high-affinity FABP7 ligands. Our protein-based approach which is not prone to false positives and also does not require any labeling of the protein should help accelerate the discovery of selective inhibitors for anandamide carrier proteins. The initial hits can then be further developed as viable molecular probes or potential drug leads for the modulation of endocannabinoid transport.

Acknowledgments

We would like to acknowledge the financial support for this research by NIH grants DA032020 (J.G.), DA003801 (A.M.), and DA009158 (A.M.) from the National Institute on Drug Abuse.

Conflict of Interest

The authors declare that there are no conflict of interests.

References

1. Devane W.A., Hanus L., Breuer A., Pertwee R.G., Stevenson L.A., Griffin G., Gibson D., Mandelbaum A., Etinger A., Mechoulam R. (1992) Isolation and structure of a brain constituent that binds to the cannabinoid receptor. Science;258:1946–1949.
2. Felder C.C., Briley E.M., Axelrod J., Simpson J.T., Mackie K., Devane W.A. (1993) Anandamide, an endogenous cannabimimetic eicosanoid, binds to the cloned human cannabinoid receptor and stimulates receptor-mediated signal transduction. Proc Natl Acad Sci USA;90:7656–7660.
3. Di Marzo V., Fontana A., Cadas H., Schinelli S., Cimino G., Schwartz J.-C., Piomelli D. (1994) Formation and inactivation of endogenous cannabinoid anandamide in central neurons. Nature;372:686–691.
4. Wilson R.I., Nicoll R. (2002) Endocannabinoid signaling in the brain. Science;296:678–682.
5. Beltramo M., Stella N., Calignano A., Lin S.Y., Makriyannis A., Piomelli D. (1997) Functional role of high-affinity anandamide transport, as revealed by selective inhibition. Science;277:1094–1097.
6. Fegley D., Kathuria S., Mercier R., Li C., Goutopoulos A., Makriyannis A., Piomelli D. (2004) Anandamide transport is independent of fatty-acid amide hydrolase activity and is blocked by the hydrolysis-resistant inhibitor AM1172. Proc Natl Acad Sci USA;101:8756–8761.
7. Fu J., Bottegoni G., Sasso O., Bertorelli R., Rocchia W., Masetti M., Guijarro A., Lodola A., Armirotti A., Garau G., Bandiera T., Reggiani A., Mor M., Cavalli A., Piomelli D. (2012) A catalytically silent FAAH-1 variant drives anandamide transport in neurons. Nat Neurosci;15:64–69.
8. Fowler C.J. (2013) Transport of endocannabinoids across the plasma membrane and within the cell. FEBS J;280:1895–1904.
9. Fowler C.J. (2014) Has FLAT fallen flat? Trends Pharmacol Sci;35:51–52.
10. Kaczocha M., Glaser S.T., Deutsch D.G. (2009) Identification of intracellular carriers for the endocannabinoid anandamide. Proc Natl Acad Sci USA;106:6375–6380.
11. Oddi S., Fezza F., Pasquariello N., D'Agostino A., Catanzaro G., De Simone C., Rapino C., Finazzi-Agro A., Maccarrone M. (2009) Molecular identification of albumin and Hsp70 as cytosolic anandamide-binding proteins. Chem Biol;16:624–632.
12. Cravatt B.F., Giang D.K., Mayfield S.P., Boger D.L., Lerner R.A., Gilula N.B. (1996) Molecular characterization of an enzyme that degrades neuromodulatory fatty-acid amides. Nature;384:83–87.
13. Furuhashi M., Hotamisligil G.S. (2008) Fatty acid-binding proteins: role in metabolic diseases and potential as drug targets. Nat Rev Drug Discov;7:489–503.
14. Balendiran G.K., Schnutgen F., Scapin G., Borchers T., Xhong N., Lim K., Godbout R., Spener F., Sacchettini J.C. (2000) Crystal structure and thermodynamic analysis of human brain fatty acid-binding protein. J Biol Chem;275:27045–27054.
15. Xu L.Z., Sanchez R., Sali A., Heintz N. (1996) Ligand specificity of brain lipid-binding protein. J Biol Chem;271:24711–24719.
16. Furuhashi M., Tuncman G., Gorgun C.Z., Makowski L., Atsumi G., Vaillancourt E., Kono K., Babaev V.R., Fazio S., Linton M.F., Sulsky R., Robl J.A., Parker R.A., Hotamisligil G.S. (2007) Treatment of diabetes and atherosclerosis by inhibiting fatty-acid-binding protein aP2. Nature;447:959–965.
17. Furuhashi M., Fucho R., Gorgun C.Z., Tuncman G., Cao H., Hotamisligil G.S. (2008) Adipocyte/macrophage fatty acid-binding proteins contribute to metabolic deterioration through actions in both

macrophages and adipocytes in mice. J Clin Invest;118:2640–2650.
18. Berger W.T., Ralph B.P., Kaczocha M., Sun J., Balius T.E., Rizzo R.C., Haj-Dahmane S., Ojima I., Deutsch D.G. (2012) Targeting fatty acid binding protein (FABP) anandamide transporters – a novel strategy for development of anti-inflammatory and anti-nociceptive drugs. PLoS ONE;7:e50968.
19. Glatz J.F.C., Veerkamp J.H. (1983) A radiochemical procedure for the assay of fatty acid binding by proteins. Anal Biochem;132:89–95.
20. Mori S., Abeygunawardana C., Johnson M.O., van Zijl P.C. (1995) Improved sensitivity of HSQC spectra of exchanging protons at short interscan delays using a new fast HSQC (FHSQC) detection scheme that avoids water saturation. J Mag Reson B;108:94–98.
21. Wu W.-J., Tyukhtenko S.I., Huang T.-H. (2006) Direct NMR resonance assignments of the active site histidine residue in *Escherichia coli* thioesterase I/protease I/lysophospholipase L1. Magn Reson Chem;44:1037–1040.
22. Oeemig J., Jørgensen M., Hansen M., Petersen E., Duroux L., Wimmer R. (2009) Backbone and sidechain ^{1}H, ^{13}C and ^{15}N resonance assignments of the human brain-type fatty acid binding protein (FABP7) in its apo form and the holo forms binding to DHA, oleic acid, linoleic acid and elaidic acid. Biomol NMR Assign;3:89–93.
23. Rademacher M., Zimmerman A.W., Ruterjans H., Veerkamp J.H., Lucke C. (2002) Solution structure of fatty acid-binding protein from human brain. Mol Cell Biochem;239:61–68.
24. Cheng Y., Prusoff W.H. (1973) Relationship between the inhibition constant (K1) and the concentration of inhibitor which causes 50 per cent inhibition (I50) of an enzymatic reaction. Biochem Pharmacol;22:3099–3108.
25. Nikolovska-Coleska Z., Wang R., Fang X., Pan H., Tomita Y., Li P., Roller P.P., Krajewski K., Saito N.G., Stuckey J.A., Wang S. (2004) Development and optimization of a binding assay for the XIAP BIR3 domain using fluorescence polarization. Anal Biochem;332:261–273.
26. Smathers R.L., Petersen D.R. (2011) The human fatty acid-binding protein family: evolutionary divergences and functions. Hum Genomics;5:170–191.
27. Young A.C., Scapin G., Kromminga A., Patel S.B., Veerkamp J.H., Sacchettini J.C. (1994) Structural studies on human muscle fatty acid binding protein at 1.4 A resolution: binding interactions with three C18 fatty acids. Structure;2:523–534.
28. Sulsky R., Magnin D.R., Huang Y., Simpkins L., Taunk P., Patel M., Zhu Y. *et al.* (2007) Potent and selective biphenyl azole inhibitors of adipocyte fatty acid binding protein (aFABP). Bioorg Med Chem Lett;17:3511–3515.
29. Muniz J.R.C., Kiyani W., Shrestha L., Froese D.S., Krojer T., Vollmar M., Arrowsmith C.H., Edwards A.M., Weigelt J., Bountra C., Von Delft F., Yue W.W. (To be published) Crystal structure of human testis-specific fatty acid binding protein 9 (FABP9). http://www.rcsb.org/pdb/explore.do?structureId=4A60, DOI:10.2210/pdb4a60/pdb.
30. Gluster J., Lewis M., Rossi M. (1994) Crystal Structure Analysis for Chemists and Biologist. New York: VCH Publishers.
31. Lucke C., Huang S., Rademacher M., Ruterjans H. (2002) New insights into intracellular lipid binding proteins: the role of buried water. Protein Sci;11:2382–2392.
32. Mayer M., Meyer B. (2001) Group epitope mapping by saturation transfer difference NMR to identify segments of a ligand in direct contact with a protein receptor. J Am Chem Soc;123:6108–6117.
33. Wagstaff J.L., Taylor S.L., Howard M.J. (2013) Recent developments and applications of saturation transfer difference nuclear magnetic resonance (STD NMR) spectroscopy. Mol Biosym;9:571–577.
34. Hajduk P.J., Olejniczak E.T., Fesik S.W. (1997) One-dimensional relaxation- and diffusion-edited NMR methods for screening compounds that bind to macromolecules. J Am Chem Soc;119:12257–12261.
35. van Dongen M.J.P., Uppenberg J., Svensson S., Lundbäck T., Åkerud T., Wikström M., Schultz J. (2002) Structure-based screening as applied to human FABP4: a highly efficient alternative to HTS for hit generation. J Am Chem Soc;124:11874–11880.